Stray light analysis of an on-axis three-reflection space optical system

Baolin Du (杜保林)[*]**, Lin Li (李　林), and Yifan Huang (黄一帆)**

School of Optoelectronics, Beijing Institute of Technology, Beijing 100081, China

[*]*E-mail: dubaolin@bit.edu.cn*

Stray light analysis of a three-mirror spatial optical system is presented. The entrance pupil diameter (EPD) of the system is 320 mm, the effective focal length (EFL) is 2809 mm, and the field of view (FOV) is $1° \times 0.5°$. Its walls are coated with extinction paint (the absorption coefficient of which is 97%). The point source transmittance (PST) of the system is thus reduced by up to two orders of magnitude. Moreover, this technique makes it feasible to block the stray light coming from outside of the FOV by increasing the outer baffle length of the system. Adding an inner baffle to both the primary and the secondary mirrors helps not only to block the stray light coming from outside of the FOV but also to decrease the length of the outer baffle. Simulation results show that the PST values are less than 10^{-10} when the off-axis angle is larger than $9°$. The stray light is also suppressed effectively by placing a glare stop at the first imaging plane of Cassegrain telescope. It is surprising that the PST value is 10^{-14} when the off-axis angle is $2°$ with the placement of glare stop at the first image plane.

OCIS codes: 080.4035, 290.1483, 290.2200, 290.2648.

doi: 10.3788/COL20100806.0569.

A three-mirror optical system can provide relaxation regarding limits on field of view (FOV) of two-mirror or one-mirror telescope[1]. Because each surface of three-mirror optical system has three parameters which are curvature, asphericity, and the mirrors spacing, nine parameters can be used to optimize the design of this system. By using these parameters, it becomes feasible to eliminate spherical aberrations, vignetting, and astigmatism. Moreover, the three reflective surfaces of the designed system share the same axis and the difficulty of alignment is greatly reduced. Therefore, the coaxial three-mirror system is widely used in space remote sensors.

Space remote sensors work in the worst environment filled with strong external radiation sources, such as the Sun, Earth, and Moon. The stray radiations from these sources will reduce the resolution of focal plane array (FPA) as well as saturate the charge-coupled device (CCD) and affect the imaging quality of the optical system[2]. To facilitate the rapid development of modern space technology, it is very important to analyze and eliminate the stray radiations during the design of space remote sensors.

Radiative transfer theory is the theoretical basis for eliminating the stray light. The radiation power reaching the detector is given as

$$\tau_{\mathrm{d}} = \tau_{\mathrm{s}} \times \mathrm{BRDF_s} \times \mathrm{GCF_{s-d}} \times \pi, \tag{1}$$

where τ_{d} is the light flux received by detector, τ_{s} is the light flux of source, $\mathrm{BRDF_s}$ means the scattering characteristic of the reflection or scattering surface, and $\mathrm{GCF_{s-d}}$ is the geometrical structure factor of the optical system. Thus, reducing each factor could reduce the stray light power reached at the detector. The stray light analysis demands that either $\mathrm{GCF_{s-d}}$ or $\mathrm{BRDF_s}$ or both should be reduced to eliminate the effect of the stray light on the optical system. We choose an ideal material for coating the sur-

face. The coating with high absorbance can reduce $\mathrm{BRDF_s}$ value of the surface. $\mathrm{GCF_{s-d}}$ value of the optical system is then reduced. It becomes feasible to reduce the $\mathrm{GCF_{s-d}}$ value by adding the stop and the baffle.

The surfaces of non-optical components of the space remote sensor are often coated with high absorbance black extinction paint. Because of this, the $\mathrm{BRDF_s}$ distribution values of surfaces will be reduced[3]. We have collected seven kinds of extinction paints which are frequently used in space optical remote sensor systems and have tested their absorbances. The seven paints are listed in Table 1[4]. Different absorbances have been observed in various extinction paints. The absorbance of the sample 7 was considered to be the best among all the seven kinds of extinction paints. It was also observed that the absorbance value of the sample 7 was the highest and the most stable in the range of visible to near-infrared bands (0.4–2 μm). Therefore, it can be used as an ideal extinction paint for the inner surfaces of space remote sensor.

In space remote sensors, such as the optical systems used for observation of the Earth or stars, space infrared optical systems, low temperature optical systems, and some large space telescopes, the bright objects (such as

Table 1. Seven Kinds of Extinction Paints

Sample	Material	Coating	Thickness (μm)
1	Titanium	Black Paint	0.5
2	Aluminium	Black Paint	1
3	Aluminium	Black Paint	5
4	Aluminium	Black Nickel	5
5	Aluminium	Black Anodization	10
6	Titanium	Black Paint	70
7	Aluminium	Black Paint	70

the Sun, the Moon, and the Earth) lying out of the FOV are the very strong external sources of stray light. Usually, the radiation intensities of these sources are several times higher in magnitude than that of the detecting target. If these stray radiations are not restrained effectively, the required image for the detector is likely to be saturated. Fortunately, it may be obtained by designing a reasonable baffle, which should assure the central obstruction ratio of the optical system as low as possible[5].

The general principles of baffle design are as follows[6]: minimizing the central obstruction as low as possible, eliminating the single stray light, and letting the stray light reach at PFA after several attenuations as much as possible. Usually, the space remote sensors consist of three major components as follows: Ritchey-Chretien (RC) telescope, scanning/folding mirror, and imaging modules. As shown in Fig. 1[7], the major role of the telescope system is to collect the maximum light flux from the outer space. Therefore, the baffle design for the telescope system is mainly accomplished by designing the outer baffle and the inner baffle. However, the inner baffle is located on the primary mirror as well as on the secondary mirror. The outer baffle is constrained by the parameters of the inner baffle, so the baffle design should be carried out first for the inner and then for the outer baffle.

The shape of inner baffles located on the primary and the secondary mirrors is often like a cone. And their major role is to block the reflection from the outer baffle and any angular incident light reaching at the focal plane. However, the length and diameter of inner baffles may be determined by the parameters of the optical system, which include the radius of curvature, eccentricity, mirror spacing, and FOV, etc.[8] The design parameters of the inner baffle are shown in Fig. 2.
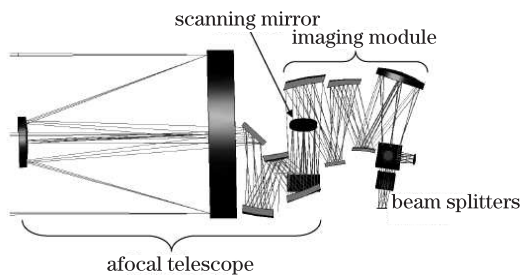

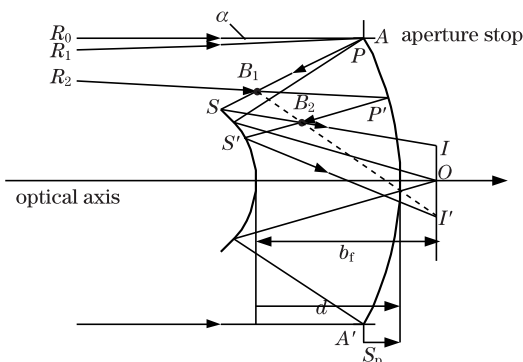Fig. 1. Structure of optical system named as WISE[7]. (WISE: wide-field infrared survey explorer).

Fig. 2. Main light path in telescope.

The FOV of the optical system is 2α, the entrance pupil AA' is set on the primary mirror. The curvature radii and eccentricities of the primary and the secondary mirrors are γ_1, ξ_1^2, γ_2, and ξ_2^2, respectively. Paralleling to the optical axis, the incident ray R_0 illuminates on the edge of the entrance pupil as well as at the edge of the primary mirror and finally reaches at the center point O of the focal plane after reflection from the secondary mirror. The ray R_1 from the edge of the entrance pupil should also reach at the edge point P of the primary mirror. Thus, the ray R_1 is the marginal ray, and it reaches at the upper edge point I of the focal plane after reflection from the secondary mirror. It is evident that the ray R_1 identifies the upper edges of the primary mirror, the secondary mirror, and the focal plane. In the same way, the ray R_2 reaches at the bottom edge point I' of the focal plane at FOV $(-\alpha)$ after reflections from the primary and the secondary mirrors. B_1 and B_2 are the intersection points on chords PS and $P'S'$ of the rays R_2 and R_1, which are the marginal points of the inner baffles of the secondary and the primary mirrors, respectively. If B_1, B_2, and I' lie on the same line, the length and the diameter of the inner baffles determined by B_1, B_2 are exact. If the extension line of B_1B_2 intersects the interior of II', the light near B_1B_2 can reach on the focal plane. On the other hand, if the extension line of B_1B_2 intersects the extension line of II', the stray incident light directly on the focal plane is blocked, but the too long baffle is not conducive to the light requirements for the remote sensors.

According to the above analysis, the formulae for the baffle design can be derived by using quadratic light path formula in the xy plane. The general equation for the incident ray is

$$y = \tan\alpha\,(x - x_0) + y_0, \qquad (2)$$

and the equation for the cross-section AA' of the primary mirror is

$$y^2 = \left(\xi_1^2 - 1\right)x^2 + 2\gamma_1 x. \qquad (3)$$

The coordinates $(s_1,\ h_1)$ of the intercept point of the incident ray on the primary mirror are given as

$$s_1 = \left(y_0 + \tan\alpha\,x_0\right)/\left(\gamma_1 + \tan\alpha\,y_0 + \tan^2\alpha\,x_0\right)\big[1 +$$
$$\sqrt{\gamma_1^2 + 2\gamma_1\tan\alpha\,(y_0 + \tan\alpha\,x_0) + (\xi_1^2 - 1)(y_0 + \tan\alpha\,x_0)^2}$$
$$/\left|\gamma_1 + \tan\alpha\,y_0 + \tan^2\alpha\,x_0\right|\big], \qquad (4)$$

$$h_1 = \tan\alpha\,(s_1 - x_0) + y_0. \qquad (5)$$

The equation of the light reflected from the primary mirror is given as

$$y = \tan\left\{2\arctan\left[h_1/\gamma_1 + \left(\xi_1^2 - 1\right)s_1\right] - \alpha\right\}$$
$$(x - s_1) + h_1, \qquad (6)$$

and the equation for the secondary mirror is given as

$$y^2 = \left(\xi_2^2 - 1\right)(x - d)^2 + 2\gamma_2\,(x - d). \qquad (7)$$

The coordinates $(s_2,\ h_2)$ of the intercept point of the

incident ray on the secondary mirror are given as

$$s_2 = [h_1 - k(d - s_1)] / (\gamma_2 + kh_1 + k^2d - k^2s_1) \left[1 + \right.$$
$$\sqrt{\gamma_2^2 + 2\gamma_2 k[y_1 + k(d - s_1)] + (\xi_2^2 - 1)[y_1 + k(d - s_1)]^2}$$
$$\left. / |\gamma_2 + kh_1 + k^2d - k^2s_1| \right], \tag{8}$$

$$h_2 = k(s_2 - s_1) + h_1, \tag{9}$$

where

$$k = \tan\left\{2\arctan\left[h_1/\gamma_1 + (\xi_1^2 - 1)s_1\right] - \alpha\right\}. \tag{10}$$

The height of the incident ray at the focal plane is

$$h_i = y_2 - (f_s + s_2)\tan\langle 2\left\{\arctan\left[h_1/\gamma_1 + (\xi_1^2 - 1)s_1\right]\right.$$
$$\left. - \arctan\left[h_2/\gamma_2 + (\xi_2^2 - 1)s_2\right]\right\}\rangle. \tag{11}$$

Equations (2)–(11) are the ray-tracing equations for the Cassegrain telescope, through which the coordinates (s, h) of the intercept points on the primary and the secondary mirrors can be obtained. Similar method is adopted to obtain the intercept height h_i at the focal plane. The subscripts 0, 1, 2 indicate the initial point, the primary mirror and the secondary mirror, respectively.

Therefore, the ray R_0 has its coordinates ($x_{00} = 0$, $y_{00} = D/2$) and its incident angle with optical axis is zero. The intercept points (s_{10}, h_{10}), (s_{20}, h_{20}) on the primary and the secondary mirrors, respectively, can easily be obtained from Eqs. (2)–(11). The intercept height h_{i0} at the focal plane can also be obtained in the same way.

The ray R_1 starts from the points at $x_{01} = s_{10}$, $y_{01} = D/2$, and its incident angle is α. The intercept points $P(s_{11}, h_{11})$, $S(s_{21}, h_{21})$ on the primary and the secondary mirrors can easily be obtained. The intercept height h_{i1} at the focal plane can also be obtained in the same way.

The ray R_2 starts from the points at $x_{02} = s_{10}$, $y_{02} = d_1$, and its incident angle is $-\alpha$, where d_1 is unknown. The intercept points $P'(s_{12}, h_{12})$, $S'(s_{21}, h_{21})$ on the primary and the secondary mirrors, respectively, can easily be obtained. The intercept height h_{i2} at the focal plane can also be obtained in the same way.

After obtaining the above mentioned quantities, we solve the intersection points of PS and R_2P' as well as SI and $S'P'$ which are indicated as $B_1(X_1, Y_1)$, $B_2(X_2, Y_2)$, respectively.

According to the optimum restriction of the length and the diameter of the inner baffle design, the points B_1, B_2, and I' should be on the same line. From this condition, we can get

$$\frac{Y_1 + h_{i2}}{X_1 - f_s + d} = \frac{Y_2 + h_{i2}}{X_2 - f_s + d}. \tag{12}$$

According to Eq. (12), we can obtain the optimal values of the points $B_1(X_1, Y_1)$ and $B_2(X_2, Y_2)$. Similarly, other parameters also have the single solutions. These parameters are the diameter $D_p = 2Y_2$ of the primary mirror baffle, the length $L_p = X_2$ of the primary mirror baffle, the diameter $D_s = 2Y_1$ of the secondary mirror baffle and the length $L_s = X_1 - d$ of the secondary mirror baffle.
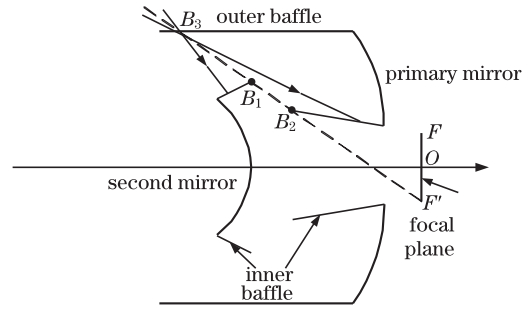

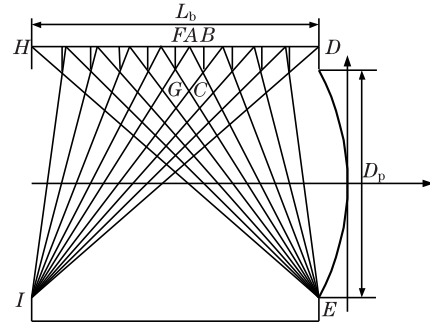Fig. 3. To solve the length of the outer baffle.

Fig. 4. Design program of vanes.

Theoretically, the longer outer baffle is more favorable to suppress the stray light. However, due to strict constraints on the size and weight of the sensors, the outer baffle cannot be extended indefinitely. To prevent the optical system from the stray radiation sources, the marginal points of the outer baffle should lie on the same line as the upper edge points of the inner baffle, as shown in Fig. 3.

It is clear from Fig. 3 that the external stray light sources radiating light from the edge point B_3 of the outer baffle at an angle greater or less than the incident angle of light ray along the dotted line will reach to the outer wall of the inner baffles. If the external stray light sources radiate light into the inner baffles along the straight line B_1B_2, the light rays will not directly reach at the focal plane due to the perfect design of the inner baffle.

The main role of vanes is to reflect, at least, twice the external radiations before reaching at the primary mirror. The extinction paint coated on the surfaces of the baffle and the vanes will help greatly to attenuate the stray radiation energy reaching at the primary mirror. In order to satisfy the condition of more than two reflections, a common design of vane is shown in Fig. 4.

In Fig. 4, L_b is the length of baffle, BC is the height of the vane, and BF is the vane spacing. According to a similar triangle theorem, we get

$$BF = \frac{L_b \times BC}{BC + D_p}. \tag{13}$$

The parameters of the optical system are $r_1 = 902.86$ mm, $\xi_1^2 = -0.953736$, $r_2 = 279.93$ mm, $\xi_2 = -2.665447$, $d = 350.44$ mm, $b_f = 361.7877$ mm, and $D = 320$ mm. From Eqs. (2)–(12), it is convenient to calculate the structural parameters of the inner baffle as follows: $D_p = 55.994$ mm, $L_p = 189.74$ mm,
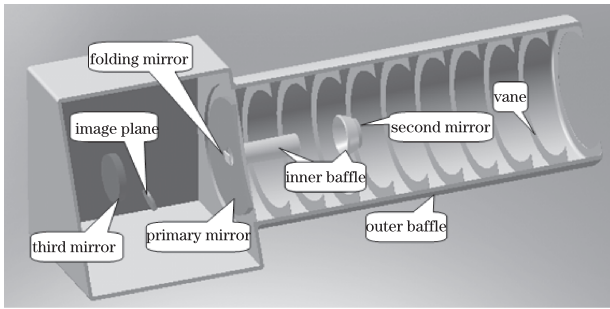
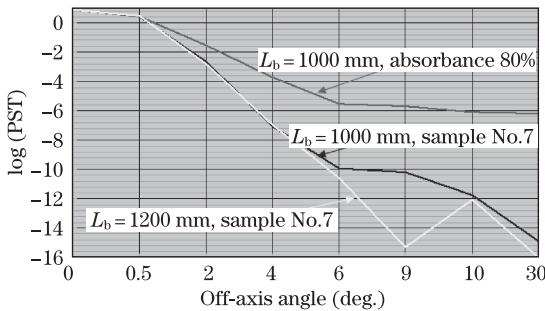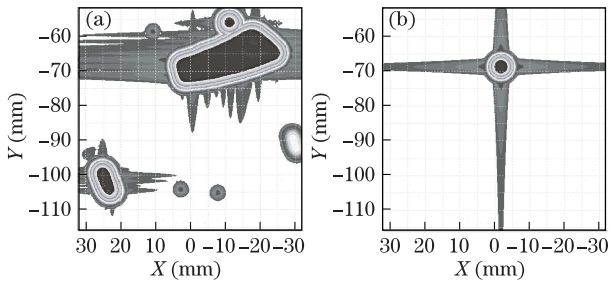Fig. 5. Profile of the system structure.

Fig. 6. PST curve.

Fig. 7. Image irradiance (a) before and (b) after adding the stop.

$D_s = 107.45$ mm, $L_s = 38.034$ mm. According to Fig. 3, using Eq. (13) and assuming the vane spacing of 100 mm, the minimum length of the outer baffle, the distance between vanes, and the height of vane are 1000, 35.55, and 100 mm, respectively. It is easy to establish the structure of the three-mirror system, as shown in Fig. 5. To compute the point source transmittance (PST) value of the system, $BSDF_s$ is assumed to be 1.3 sr^{-1} and the chosen extinction paint is sample 7 whose absorbance is

97%. Figure 6 shows the PST curve of sample 7.

As shown in Fig. 6, the longer outer baffle and the higher absorbance of the extinction paint have better effect on the suppression of stray light. The curve of L_b = 1200 mm rises at 10°, which is caused by some stray light scattered by the vanes near the entrance of the outer baffle into the FOV. It can be prevented by optimizing the array form of vanes. It is also observed that the two PST curves marked with sample 7 can achieve the order of magnitude of 10^{-10} when the off-axis angle is greater than 9°. Taking into account the first image of Cassegrain telescope, it is effective to suppress the stray radiation from telescope by placing a glare stop at the first image. This makes the PST hit the order of magnitude of 10^{-14} when the off-axis angle is 2° after adding stop. Figure 7 shows the difference of the image irradiance when the off-axis angle is 2° before or after adding the stop.

In conclusion, the analysis of stray radiation for a space remote sensor is proposed. It is proved that the stray light level of the remote sensor is affected by three important factors. They are extinction paint, the length of baffle, and the location of stop. It is also worth noting that adding an inner baffle on the primary and the second mirrors reduces the length of outer baffle without reducing the stray light performance of remote sensors.

References

1. M. Lampton and M. sholl, Proc. SPIE **6687,** 66870S (2007).
2. J. Wang, S. Wang, and G. Lin, Chin. Opt. Lett. **6,** 510 (2008).
3. C. Qi, C. Yang, W. Li, and J. Dai, Chin. Opt. Lett. **1,** 398 (2003).
4. B. Du, L. Li, Y. Huang, Y. Zhao, and Z. Jiang, Acta Photon. Sin. (in Chinese) **37,** (S2) 220 (2008).
5. J. C. Fleming, Proc. SPIE **3779,** 353 (1999).
6. N. Song, X. Han, and R. Li, Acta Opt. Sin. (in Chinese) **20,** 821 (2000).
7. A. K. Mainzer, P. Eisenhardt, E. L. Wright, F.-C. Liu, W. Irace, I. Heinrichsen, R. Cutri, and V. Duval, Proc. SPIE **5899,** 58990R (2005).
8. V. Y. Terebizh, Experimental Astronomy **11,** 171 (2001).